Electron-impact dissociation of nitrogen

Cite as: J. Chem. Phys. **98**, 9544 (1993); https://doi.org/10.1063/1.464385
Submitted: 03 February 1993 . Accepted: 12 March 1993 . Published Online: 31 August 1998

P. C. Cosby

Electron-impact dissociation of nitrogen

P. C. Cosby
Molecular Physics Laboratory, SRI International, Menlo Park, California 94025

(Received 3 February 1993; accepted 12 March 1993)

The electron-impact dissociation of N_2 to form two nitrogen atoms is observed in a crossed beam experiment at electron energies between 18.5 and 148.5 eV. Detection of the correlated dissociation fragments with a time and position sensitive detector permits detection of both ground and excited state fragments, but excludes interference from dissociative ionization products. The observed translational energy releases in the N_2 dissociation are consistent with predissociation to $N(^2D)+N(^4S)$ fragments as the primary dissociation mechanism. Absolute cross sections for the electron impact dissociation are measured and compared with previous measurements. Recommended values of this cross section are given for electron-impact energies between 10 and 200 eV.

INTRODUCTION

The nitrogen molecule comprises a significant fraction of the Earth's atmosphere and the atmospheres of Titan and Triton. Within these environments, N_2 is subject to significant bombardment both by energetic electrons, as is characteristic of aurorae, and by lower energy photoelectrons produced in the normal atmosphere.[1] Ionization,[2–4] dissociative ionization,[5–7] excitation,[8] and dissociation[9–12] of the N_2 can result from electron impact. Laboratory studies have produced a rather complete set of quantitative data[13] for these processes, with the exception of electron impact dissociation. In the electron-impact dissociation reaction

$$N_2+e^-\rightarrow N_2^*+e^-\rightarrow N+N+W+e^-, \qquad (1)$$

electron impact produces an electronically excited state of N_2 that subsequently dissociates into atoms with the release of translational energy, represented here by W. While the overall cross section for this reaction is known,[8,13] little information is available concerning the electronic states and translational energies of the products which determine their subsequent reactions.[14]

Electron energy loss studies[15–18] have shown that discrete (bound) levels of N_2^* are produced in the first step of reaction (1); thus dissociation of N_2 must primarily occur through predissociation. Only three electronic states of the atoms, ^4S, ^2D, and ^2P, are energetically accessible below the ionization limit of the molecule, but an *a priori* prediction of the branching among these in the predissociation is greatly complicated by strong Rydberg–valence interactions[19] among the N_2^* levels, as evidenced by experimental measurements in a small fraction of the relevant levels.[20] Measurements have been made of the concentrations of $N(^2D)$ and $N(^2P)$ in the upper atmosphere,[21,22] but many processes other than reaction (1) contribute to these observations.

The present measurements observe reaction (1) in a crossed beam arrangement in which an electron beam intersects a fast beam of N_2. The spatial and temporal separations of the correlated pair of atomic products formed in the dissociation of a single N_2 molecule are explicitly measured to provide a direct measurement of the translational energy release W in reaction (1). The measured translational energy release, in combination with the known energies of N_2^*, also determines the electronic states of the dissociation products. Detection of charged products is explicitly excluded in the experiment, allowing the electron impact dissociation products of N_2 to be detected without contamination from dissociative ionization processes. Quantitative product detection further allows an independent measurement of the cross section for reaction (1) over the electron energy range of 18.5 to 148.5 eV.

EXPERIMENT

The experimental apparatus and measurement procedures have been described in detail for the electron-impact dissociation of CO (Ref. 23) and will be considered only briefly here. A fast (3–5 keV), collimated beam of N_2 molecules is created by near-resonant charge transfer neutralization of an N_2^+ beam and intersected at right angles by an electron beam within an interaction region defined by a narrow slit and a beam flag. Undissociated molecules are collected by the beam flag. If an N_2 molecule dissociates within this region and its fragments are produced with sufficient transverse velocity to escape collection by the beam flag, the correlated pair of fragments is detected by a position sensitive detector (PSD-C) which measures their radial (R) and temporal (Δt) separations.[24] This measurement specifies the center-of-mass translational energy released in the dissociation (W), i.e., the difference in energy between the dissociating molecular state and its atomic products at infinite separation[25]

$$W=\frac{E_0}{4L^2}\left[R^2+\left(\frac{2E_0\Delta t}{M}\right)^2\right]. \qquad (2)$$

Here the translational energy of the fast N_2 beam, E_0, is taken to be the energy of the N_2^+ precursor in the charge transfer, L is the distance between the point of dissociation of the N_2 molecule and the PSD-C, and M is the mass of the N_2 molecule. These are taken to be constants describing all dissociating N_2 molecules. The measurement further specifies the angular distribution of the fragments in the

 0021-9606/93/129544-10$06.00

planes orthogonal to the detector. The fast N_2 beam flux is measured by a pyroelectric bolometer and the absolute collection efficiency of the PSD-C for dissociation fragments is calibrated. All charged particles are collected by a weak electric field in the region between the beam flag and the PSD-C; hence dissociative ionization products do not contribute to the present measurements.

As described previously,[23] the electron beam has a rectangular geometry and an energy spread of ~ 1.5 eV FWHM. Energy calibration of the electrons is made from the observed threshold for the ionization of Ar (Ref. 26) and has an estimated accuracy of ± 1 eV. Overlap between the electron and neutral beams is controlled by physically translating the electron gun and electron collector as a unit. This capability allows distinction to be made between neutral fragments created by spontaneous or collisional dissociation of the N_2 in the region between the slit and the beam flag, and electron impact dissociation of N_2 within the electron beam. The gun translation further allows an accurate dissociation cross section to be measured without a specific determination of the form factor describing the overlap of the electron and neutral beams.

With the electron gun and the neutral beam aligned, overlap of the beams takes place within a $\Delta L = 2.6$ cm interval along the neutral beam flight path. Since it is not known *a priori* where along this interval a particular N_2 molecule dissociates to produce a detected pair of fragments, the value of W implied by Eq. (2) can deviate from the true magnitude of the translational energy release by the factor

$$\frac{\Delta W}{W} = \frac{2\Delta L}{L} = 0.052. \tag{3}$$

This factor represents the effective translational energy resolution achieved by the PSD-C for the electron-impact dissociation fragments. Pressures within the interaction region were maintained at $< 2 \times 10^{-8}$ Torr during the measurements.

Two orientations of the electron beam velocity vector with respect to the PSD-C in combination with the fragment angular distribution observed by the PSD-C are required to define the full angular distribution of the electron-impact dissociation fragments. In the present measurements, these distributions are found to be isotropic within the center-of-mass frame of the N_2 at electron-impact energies $\geqslant 28.5$ eV. At lower electron energies, the flux of fragments dispersed in both energy release and angle was too small for a detailed angular distribution to be determined. In interpreting the present data, we presume that this distribution remains isotropic at lower electron energies.

The state distribution of the fast N_2 beam at the time of electron impact is primarily dependent on the distribution in the N_2^+ precursor. Measurements were made for the N_2^+ produced in two different ion sources: a hollow cathode discharge source[27] (HC) and an electron-impact ionization source[28] (EI). The EI source was operated with low pressure ($\sim 10^{-4}$ Torr) N_2 gas and 100 eV ionization energy. Electron impact on N_2 at this energy populates three electronic states of N_2^+: $X\,^2\Sigma_g^+$, $A\,^2\Pi_u$, and $B\,^2\Sigma_u^+$ with relative abundances of 0.5, 0.4, and 0.1 respectively.[4] The B state is short-lived[13] and radiates primarily into the $X\,^2\Sigma_g^+$ state inside the ion source volume. However, the A state is relatively long lived, with vibrationally dependent lifetimes[29] ranging from 16.0 μs in $v=0$ to 7.6 μs in $v=7$, and radiates into the X state throughout the 6.4 μs flight time between the ion source and the charge transfer cell. The population distribution in the N_2^+ beam at the time of charge transfer is estimated[23] using the ionization Franck–Condon factors for the initial vibrational distribution in each of the N_2^+ electronic states and Einstein A factors for the radiative decay into the ion ground state, both taken from the recent evaluation of Gilmore *et al.*[29] These predict 76% of the ion population in the $X\,^2\Sigma_g^+$ state, 80.6% of which is in $v=0$, 13.9% in $v=1$, and the remainder in higher levels. The remaining 24% of the ion beam resides in the A state, 93% of which is distributed among $0 \leqslant v \leqslant 3$.

In the hollow cathode discharge in N_2 gas at pressures in the range of 0.5–1.0 Torr, the nascent ionization products are subject to numerous low energy ion molecule reactions before leaving the source. Successive charge transfer reactions, in particular, lead to a net electronic and vibrational relaxation of the molecular ions into their ground state. This has been verified experimentally[28,30] in the case of O_2^+ and H_3^+ production and is expected to also be the case for N_2^+. It is anticipated that $>90\%$ of $N_2^+(\mathrm{HC})$ populates the $X\,^2\Sigma_g^+(v=0)$ level.

The product distributions formed in the charge-transfer neutralization of N_2^+ at keV energies in N_2 gas are governed by the Franck–Condon factors for the ionization/recombination transitions in the exchange and by a propensity to retain thermoneutrality in the reaction for production of the forward scattered products. For the symmetric charge exchange reaction

$$N_2^+(X,v') + N_2(X,v=0) \rightarrow N_2(X,v'') + N_2^+(X,v) \tag{4}$$

the partial cross sections have been calculated[31,32] for specific values of v' and v''. These predict that neutralization of $N_2^+(\mathrm{HC})$ will produce a fast N_2 beam with $\sim 90\%$ of its population in $X\,^1\Sigma_g^+(v=0)$. For the case of $N_2^+(\mathrm{EI})$, reaction (4) is expected to yield significant populations in both $v=0$ and $v=1$ of $X\,^1\Sigma_g^+$. However, this distribution is augmented by both symmetric and asymmetric charge transfer channels from the large fraction of $N_2^+(A)$ in the beam, which will undoubtedly yield a higher degree of vibrational excitation, extending at least to $v''=5$, in the product N_2 beam. However, the contribution of this vibrational excitation to the final beam depends critically on the relative charge transfer cross sections of $N_2^+(X)$ and $N_2^+(A)$ with N_2, since $\leqslant 10\%$ of the N_2^+ beam is actually neutralized under the conditions of the experiment. A smaller relative charge transfer cross section for $N_2^+(A)$ in N_2 was indicated by the experimental measurements of Flannery *et al.*[31] This is consistent with the fact that reaction (4) involves the capture of an electron into the $3\sigma_g$ orbital of the N_2^+ core, whereas neutralization of $N_2^+(A)$ involves capture into the $1\pi_u$ orbital. Preferential capture into the $3\sigma_g$ orbital of O_2^+ is found to dominate in $O_2^+ + Cs$

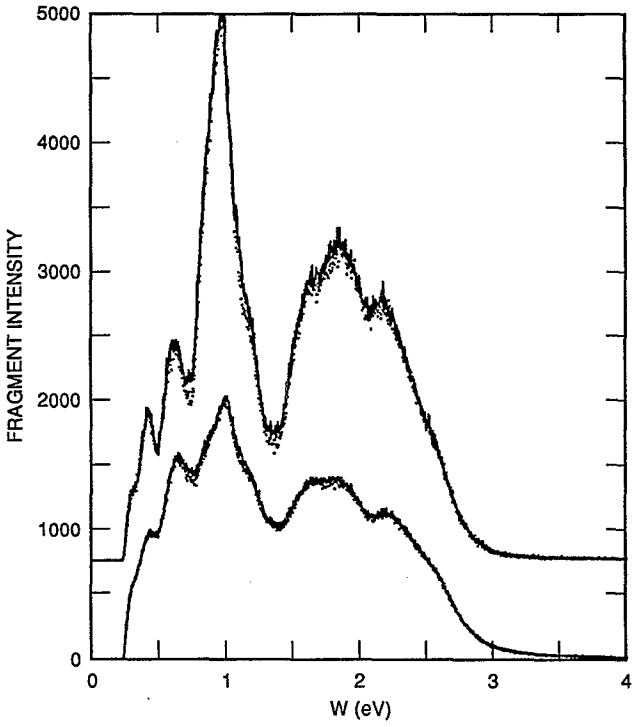

FIG. 1. Distribution of translational energy releases W observed for the dissociation of N_2. The spectra are uncorrected for the variation in the collection efficiency of the apparatus with W. Distributions in the lower part of the figure are observed for an N_2 beam produced from neutralization of N_2^+ formed in the hollow cathode ion source. A low pressure electron-impact source was used to generate the precursor N_2^+ for the distributions in the upper part of the figure. Fragment distributions observed with the electron beam intersecting the N_2 beam are shown by the solid lines, while those observed with no intersection between the electron and N_2 beams are given by the points.

reactions.[33] Thus vibrational populations in $v''>1$ of the N_2 beam formed from N_2^+(EI) should not exceed 24% of the beam, and will likely comprise a substantially smaller fraction of the beam population.

RESULTS

Fragment energy distributions

Dissociation of N_2 is found to occur not only as a result of electron-impact excitation, but also from the unimolecular dissociation of excited states populated during production of the fast N_2 beam. Representative distributions of fragment translational energy release (W) observed for a 3000 eV N_2 beam are shown in Fig. 1. In accumulating these distributions, the value of W was calculated from Eq. (2) given the observed values of R and Δt of each detected dissociation fragment pair, assuming a fixed value for L corresponding to the distance from the center of the electron beam to the detector, and assuming an N_2 beam energy E_0 equal to the acceleration potential of the N_2^+ precursor. Based on this calculated value of W and the position of the electron beam relative to the N_2 beam, the event is binned into one of two sets of 1024 equally spaced W intervals in the range $0 \leqslant W \leqslant 5.0$ eV. The histograms represented by the solid lines in Fig. 1 were obtained with the electron beam intersecting the N_2 beam, while those represented by discrete points were observed when the electron beam was positioned such that no intersection of electrons with the N_2 beam was possible. These distributions are uncorrected for the collection efficiency of the apparatus, which produces the apparent cut off in fragment intensity near $W=0.2$ eV. They reflect N_2 dissociation products that were formed somewhere within the 18 cm long interaction region defined by the slit and the beam flag (see Fig. 1 of Ref. 23), i.e., to dissociations that occurred during the interval 2.7–4.0 μs after the charge transfer formation of the N_2. The distributions are also not corrected for resolution, Eq. (3), which for $\Delta L=18$ cm is significantly degraded for dissociation processes that occur throughout this region ($\Delta W/W=0.37$). The upper distributions in Fig. 1 are obtained from an N_2 beam formed from N_2^+(EI) with a total accumulation time of 4.6 h, equally divided between electron beam intersection and nonintersection using a 1.1 mA beam of 48.5 eV electrons and an N_2 beam flux of 4×10^9 s^{-1} in the interaction region. The lower set of distributions in Fig. 1 were observed with the N_2 beam formed from N_2^+(HC). These spectra were acquired over a longer time interval and at a lower electron energy (30 eV) and current, but are scaled in the figure to the same product of N_2 beam flux and accumulation time as is appropriate for the upper distributions.

Spontaneous dissociation fragments

Dissociation of N_2 in the absence of electron beam interaction represents a rather substantial background to observing the N_2 electron impact dissociation products, indicated by the small intensity difference between the solid lines and the dots in Fig. 1. Under the conditions of the present measurements, the background dissociation represented >95% of the observed fragmentation. This background is independent of pressure within the interaction region, suggesting that it arises from unimolecular dissociation of electronically excited N_2^* molecules in the beam. The structure in the W distribution of this background, reflecting the energetic locations of the dissociating N_2^* electronic states relative to their separated atoms, appears quite similar for both N_2^+(EI) and N_2^+(HC) precursors, qualitatively suggesting that essentially the same dissociating N_2^* states are formed. However, the relative intensities of specific features are substantially greater when the N_2^+ is produced by electron impact, presumably reflecting an increased cross section for their charge transfer formation from the $A\,^2\Pi_u$ state. Furthermore, the overall intensity of spontaneous dissociation is greater in the N_2 beam formed from the N_2^+(EI) precursor, representing a fractional decay of 5×10^{-6} of the N_2 beam flux within the interaction region, compared with a fractional decay of 2×10^{-6} for N_2 formed from N_2^+(HC). Explicit identification of the dissociating N_2^* states solely on the basis of these W distributions is difficult because of the very poor resolution, $\Delta W/W\sim0.37$, that accompanies the very long region over which products are collected, and is beyond the scope of the present paper. However, fragments produced in the

region near $W=2$ eV have been optically identified as arising from predissociation of the metastable $a''\,{}^1\Sigma_g^+(v=0)$ level.[34] Given the known lifetime[35] of this state ($3.49 \pm 0.10\,\mu s$) and the range of flight times between the charge transfer cell and the interaction region, we can estimate the concentration of $a''\,{}^1\Sigma_g^+(v=0)$ in the nascent N_2 beam to be approximately 10 ppm from the observed flux of fragments. Such a small population would be consistent with the fact that a'' formation by charge transfer in N_2 is approximately 12 eV nonresonant. Lifetimes of the other states contributing to the spontaneous background dissociation are not known, but the formation of these states would also be highly nonresonant; hence it is reasonable to assume that their fractional concentration in the N_2 beam is also quite small.

Electron-impact dissociation fragments

Despite the relatively high flux of spontaneous dissociation fragments, the W distribution of the electron-impact dissociation process, Eq. (1), can be obtained from a direct subtraction of the nonintersecting W distribution from the distribution obtained with the electron beam intersecting the N_2 beam. These distributions, now corrected for the collection efficiency of the apparatus and binned into 1/15 fewer W intervals to minimize the statistical error introduced by the subtractions, are shown in Fig. 2. The statistical error associated with each binned intensity is represented by its error bar in the figure. Fragment intensities within each bin are connected by a solid line to assist a visual identification of the fragment intensity in adjacent W bins. It should be noted that the size of each bin in the distribution exceeds the nominal resolution of the apparatus for energy releases $W<1.2$ eV, as indicated by Eq. (3). The true collection efficiency for fragments produced with $W<0.5$ eV is strongly dependent on the precise alignment of the beam collection flag with the N_2 beam. Error bars given for those points in the distribution at these low values of W may therefore not fully reflect the actual magnitudes of the errors. Because of the relatively large spontaneous dissociation background, the statistical errors throughout the distribution are quite large. Nevertheless, a clear pattern of structure appears in the distributions that is reproducible and varies little with changes in electron-impact energy, or with the choice of bin size. This is indicated by the three distributions shown in Fig. 2.

The top and center distributions in Fig. 2 are observed for an N_2 beam produced from N_2^+(HC) with electron impact energies of 28.5 and 48.5 eV, respectively. The bottom distribution is obtained at an electron impact energy of 48.5 eV for the N_2 beam produced from N_2^+(EI). It can be seen that for each of these distributions, the highest fragment intensities are produced in two peaks centered near $W\sim0.8$ and $W\sim1.1$ eV. Substantial fragmentation also occurs at lower energy releases and for energy releases $W<2.4$ eV. At higher values of W, the fragmentation intensity is much smaller, despite the fact that the sensitivity of the apparatus is quite uniform for fragments produced with energy releases in the range 1 eV$\leqslant W\leqslant$3 eV. The fragment distributions shown for the two electron energies in Fig. 2 are also characteristic of those observed at higher electron impact energies. At electron energies below $\sim$25 eV, it was not possible to obtain a statistically significant distribution of fragment flux dispersed among a useful

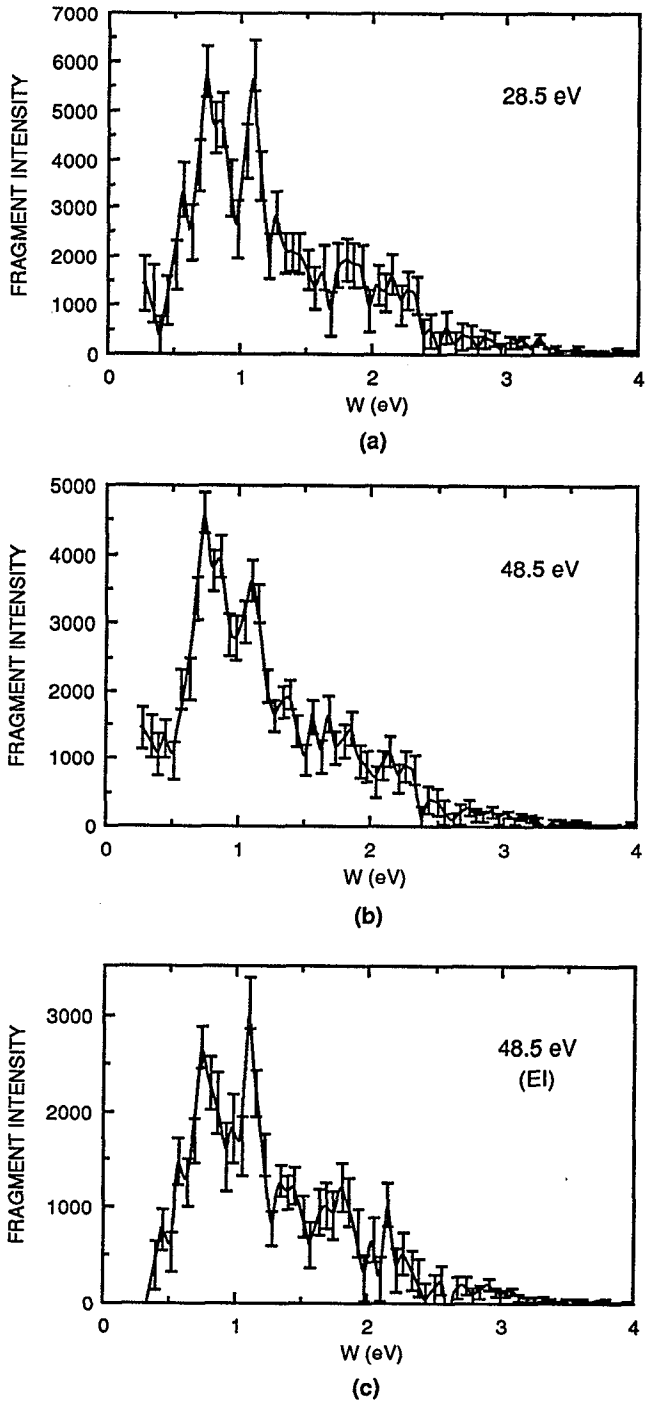

FIG. 2. Translational energy release distributions produced by electron-impact dissociation of N_2. The distributions have been corrected for collection efficiency, but not for the variation in resolution with W [see Eq. (3)]. Distributions at the top and center of the figure are observed for electron impact energies of 28.5 and 48.5 eV, respectively. The distribution at the bottom of the figure is observed for 48.5 eV electron impact on an N_2 beam with enhanced vibrational excitation. Statistical errors of the points in the three distributions are represented by the error bars. The solid lines are included only as a guide to interconnect discrete points in the distributions.

number of W bins, due to the decrease in both electron beam intensity and dissociation probability with decreasing electron energy.

As noted above, fragmentation in the range of $0.5 \leqslant W \leqslant 1.2$ eV groups into at least two peaks which are quite narrow. Such a distribution is characteristic of the predissociation of discrete energy levels in the N_2, rather than the result of an electron-impact excitation to a dissociative continuum. Predissociation is also found to characterize the fragment energy distributions observed in the electron-impact dissociation of the isoelectronic CO molecule.[23] Despite the rather large error bars, the $W \sim 1.1$ eV peak is clearly narrower than that centered near $W \sim 0.8$ eV and has a peak intensity comparable to or smaller than the $W \sim 0.8$ eV peak for the N_2 beam formed from N_2^+(HC). There is also a suggestion of subsidiary structure in the $W \sim 0.8$ eV peak. The variation in fragmentation intensity with W is more regular at the higher energy releases. However, the degradation in energy resolution with increasing energy does not allow a clear distinction between the production of these fragments by continuum dissociation or by the predissociation of several N_2 energy levels. At fragment energy releases below $W \sim 0.5$ eV, the fragment distributions are less reproducible, for the reasons given above and show no clear evidence of structure. The data do indicate, however, that the flux of fragments in this region is consistently higher from beams produced from the neutralization of N_2^+(HC) than from N_2^+(EI), although in each case, these low energy fragments represent a relatively small fraction of the total dissociation products.

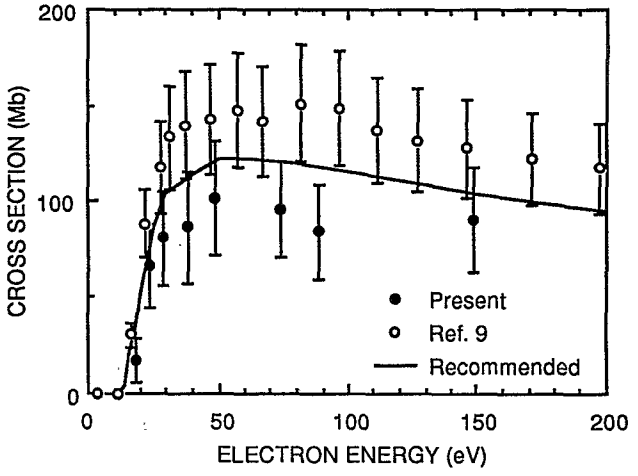

FIG. 3. Cross sections for electron-impact dissociation of N_2 [reaction (1)]. Present measurements are given by the filled circles together with error bars indicating the estimated absolute uncertainty. The previous measurements of Ref. 9, corrected for dissociative ionization, are given by the open circles. The solid line connects the recommended values for the cross section listed in Table II.

Dissociation cross section

The total dissociation cross section σ_{dis} is obtained from the relation

$$\sigma_{\text{dis}} = \frac{N^* u v_n \eta e}{\xi \chi I_e I_{fc}}, \qquad (5)$$

as discussed in Ref. 23. Here I_{fc}/η is the N_2 beam flux, I_e is the electron beam current, v_n is the velocity of the N_2 beam, taken here to be the velocity of the N_2^+ precursor, e is the electron charge, ξ is the coincidence efficiency of the PSD-C, and χ is the collection efficiency of the PSD-C, i.e., the fraction of the total cm distribution of the dissociation fragments that is viewed by the detector, and N^* is the total accumulated number of electron impact dissociation pairs as the electron beam is slowly translated completely across the N_2 beam at a constant velocity u. Each of these terms is separately measured with the exception of the PSD-C collection efficiency χ, which is an explicit function of the N_2 beam energy, fragment energy release W, and the center of mass angles Θ and Φ defining the ejection of the fragments orthogonal to the plane of the PSD-C and within the plane of the PSD-C, respectively. Only Θ is explicitly measured by the PSD-C for each dissociation event, whereas the Φ distribution must be inferred from a comparison of the total apparent cross sections measured at two different orientations of the electron beam with respect to the active axis of the PSD-C. Thus χ makes the single largest contribution to the uncertainty in σ_{dis}. Finally, an error is introduced into the cross sections by the present inability to observed fragments produced with $W < 0.3$ eV. As can be seen in Fig. 2, there is appreciable fragment flux at values of W just above this limit, particularly when the N_2 beam is formed from N_2^+(HC). However, as discussed in the next section, there is no reason to believe that very low energy releases would dominate the electron-impact dissociation for this molecule. For the present measurements, we approximate this unobserved flux by extrapolating the average fragment intensity observed for the interval $0.3 \leqslant W \leqslant 0.5$ eV to $W = 0$. This introduces an increase in fragment flux beyond that actually observed of roughly 5%. The total absolute uncertainty in the dissociation cross section, taken as the rms sum of the uncertainties in Eq. (5), is $\pm 28\%$.

The absolute cross section for electron-impact dissociation of N_2, reaction (1), was measured over the electron energy range of 18.5 to 148.5 eV using an N_2 beam formed from N_2^+(HC). The measured values, in units of megabarns ($1\ \text{Mb} = 1 \times 10^{-18}\ \text{cm}^2 = 0.01\ \text{Å}^2$) are shown by the solid points in Fig. 3 and are given in Table I as a function of electron impact energy. The estimated absolute errors in these values are given in Table I and are represented by the bars in Fig. 3. Dissociation cross sections were also measured at several electron-impact energies using an N_2 beam formed from the N_2^+(EI) precursor. No detectable systematic difference in the cross section values from those given in Table I was observed.

The dissociation cross section of N_2 has also been determined by Winters[9] from measurements of the effective pumping speed within a constant volume of N_2 gas that is produced by the adsorption of the N-atom dissociation products on nickel and molybdenum surfaces following electron impact. This measurement included not only

TABLE I. Cross sections (σ_{dis}) measured for the electron-impact dissociation of N_2. The dissociative ionization cross section from Ref. 13 has been subtracted from the measured cross section of Ref. 9 to arrive at the values labelled Winters. Cross section units are 1 Mb$=1\times10^{-18}$ cm^2.

Electron energy (eV)	Dissociation cross section (Mb)		
	Present measurements		Winters
	σ_{dis}	Uncertainty	σ_{dis}
18.5	17.4	11.4	54.2
23.5	66.5	22.0	98.5
28.5	80.7	24.7	121.3
38.5	86.5	29.0	139.9
48.5	101.7	29.5	143.3
73.5	95.5	25.2	146.0
88.5	84.0	25.1	150.2
148.5	90.2	27.2	127.2

electron-impact dissociation, reaction (1), but also dissociative ionization

$$N_2+e^-\rightarrow N^+ +N+2e^-. \quad (6)$$

However, the cross section for reaction (6) has been independently measured by several groups[5,6,13] as a function of electron energy. If we subtract this dissociative ionization cross section, using the recommended values of Itikawa *et al.*,[13] from the dissociation cross section of Winters, the cross section for reaction (1) is obtained. These values are shown by the open circles in Fig. 3 and are also listed in Table I. The error limits given in Fig. 3 are the absolute errors of $+10\%/-20\%$ estimated by Winters (but shown in the figure as $\pm20\%$), and do not include the small additional errors associated with the dissociative ionization cross section. A comparison of the solid and open circles in Fig. 3 shows that the present measurements lie uniformly below the implied measurements of Winters. However, it is also seen in this figure that with few exceptions, both sets of measurements overlap within their stated error limits. One exception is the cross section at an electron impact energy of 18.5 eV, where the present measurement has a value of roughly 32% that of the interpolated value of Winters. However, in this region, the cross section changes rapidly with electron energy, hence systematic errors in the electron energy of the two data sets (±1 eV in the present measurements) will appear as a difference in cross section magnitude. Also, the angular distribution of fragments could not be explicitly determined in the present measurements at this low electron energy; rather it was assumed that it remained constant from observations at higher energies. This introduces an increased uncertainty because molecular alignment will likely be enhanced as the excitation threshold is approached. Since the dissociation cross section for N_2 obtained in the present measurements and the value of this cross section implied by the measurements of Winters are reasonably consistent within their state error limits, the best estimate for the dissociation cross section of N_2 would be obtained from an average of the two sets of measurements.

TABLE II. Recommended cross section for the electron-impact dissociation of N_2. Cross section units are 1 Mb$=1\times10^{-18}$ cm^2.

Electron energy (eV)	Estimated cross section (Mb)	Probable absolute uncertainty (Mb)
10	0	
12	1	
14	4	
16	20	
18	36	18
20	52	20
25	87	17
30	104	22
40	115	26
50	123	21
60	123	24
80	120	30
100	116	30
125	110	22
150	104	18
175	99	
200	95	

Neither the present measurements nor the measurements of Winters gives a good definition of the variation of the dissociation cross section with electron energy in the immediate region of the dissociation threshold. However, detailed relative cross sections in this region have been reported by Winters, Horne, and Donaldson,[36] who also used a surface adsorption measurement technique, and also by Niehaus.[10] The latter work utilized a pair of modulated electron beams and mass spectrometer detection to observe the neutral products of electron impact dissociation. A significant variation of this method has recently been used[37] to determine the electron impact dissociation cross section of CH_3. The sensitivity of Winters *et al.*'s experiment to variations in the fragment angular distribution near threshold should be minimal, but that of Niehaus is unclear. Nevertheless, Zipf[38] has noted that the relative cross sections of Winters *et al.* and Niehaus are in good agreement, suggesting that these relative cross sections are reliable.

An improved representation of the cross section for electron-impact dissociation of N_2 can be obtained by taking a weighted average of the present absolute cross section values and those of Winters[9] and extrapolating this average to threshold electron impact energies using the relative pumping speed measurements of Winters, Horne, and Donaldson.[36] Derived values for this cross section are given in Table II for electron energies between 10 and 200 eV and are shown by the solid line in Fig. 3.

DISCUSSION

Because of the importance of N_2 in the earth's atmosphere, where it is subject to electron impact by ambient photoelectrons and auroral electrons, the excitation and dissociation of N_2 has received considerable attention. Excitation processes have been particularly well characterized over the past 30 years using the technique of electron energy loss spectroscopy. Although discrepancies exist in the

excitation cross sections of particular electronic states which are being addressed even at the present time,[39] the identification and relative importance of most N_2 electronic states excited by electron impact is reasonably well understood. The ultimate fate of these excited states, however, is considerably less clear. Despite a rather substantial bond dissociation energy[40] of 9.7537 ± 0.0011 eV, most of the electronic states in N_2 lie above the lowest dissociation limit $N(^4S)+N(^4S)$. Thus the possible decay channels of the excited states includes not only radiative cascade to lower states, but also predissociation to atoms and, above $15.580\,732 \pm 0.000\,009$ eV, ionization.[41] The problem is more complex yet, when one considers that for 50 eV electron impact, at least 80% of the electronic excitation to states above the first dissociation limit populates the bound states $b\,^1\Pi_u$, $b'\,^1\Sigma_u^+$, $c\,^1\Pi_u$, $c'\,^1\Sigma_u^+$, $c\,^1\Pi_u$, $e\,^1\Pi_u$, and $e'\,^1\Sigma_u^+$ states.[8] All vibrational levels of these states lie above the second N_2 dissociation limit, $N(^2D)+N(^4S)$ at 12.1373 eV, and many of their levels also lie above the third limit, $N(^2P)+N(^4S)$ at 13.329 eV. Thus predissociation to two or three dissociation limits can compete with allowed optical fluorescence into the ground $X\,^1\Sigma_g^+$ state or the $a\,^1\Pi_g$ state. In addition, the b and b' valence states are strongly mixed with the c, c', o, e, and e' Rydberg states.[19] This mixing produces large irregularities in the spacings of the rovibrational levels and in transition intensities. Furthermore, it produces irregularities in both predissociation rates and product branching ratios since the mixing implicitly modifies the coupling to the dissociation continua.

Dissociation of N_2 has been considered in detail by Zipf and McLaughlin.[11] They measured the cross sections for the emission of photons from these states as a function of electron energy. By subtracting the emission cross sections from the excitation cross sections derived from electron scattering data,[15] they arrived at state specific dissociation cross sections and predissociation branching ratios (η_{dis}, the ratio of the predissociation cross section to the excitation cross section) for individual vibrational levels in the N_2 states. Their data, summarized by electronic state for 200 eV electron impact, is given in Table III. More recently, Ajello *et al.*[12] have measured the emission cross sections at higher resolution utilizing the recent reevaluation[42] of the Lyman-α cross section which serves as the vuv emission standard in both their and earlier work. They also derive cross sections for the predissociation of individual vibrational levels by subtracting the measured emission cross sections from electron impact excitation[8] cross sections. Their results for the N_2 states, as summarized by James *et al.*[43] for 100 eV electron impact, are also given in Table III, as are the excitation cross sections for these states at 50 eV given by Trajmar *et al.*[8] A comparison of the measurements in Table III shows first that there is considerable variation in the values of the excitation cross sections assumed for the various states. This variation is even more pronounced when one considers that the cross sections for each of these states should decrease as the electron energy increases from 100 eV to 200 eV. Despite this variation, there is a remarkable degree of consistency

TABLE III. Partial excitation cross sections and dissociation fractions (η_{dis}) for the electronic states of N_2.

	Excitation cross section (Mb)			η_{dis}	
State	Ref. 11 200 eV	Ref. 43 100 eV	Ref. 8 50 eV	Ref. 11 200 eV	Ref. 43 100 eV
$a\,^1\Pi_g$		6.2[a]	2.9		0.12[a]
$w\,^1\Delta_u$			0.7		
$b\,^1\Pi_u$	20.7	12.1	17.8[b]	0.97	0.95
$b\,^1\Sigma_u^+$	17.1	12.8	10.3[b]	0.83	0.84
$c\,^1\Pi_u$	12.0	16.1	8.7[b]	>0.99	1.0
$c\,^1\Sigma_u^+$	23.8	12.1	12.5[b]	0.29	0.0
$o\,^1\Pi_u$	4.8	7.5	2.1[b]	>0.99	1.0
$e\,^1\Pi_u$	2.0			>0.99	
$e\,^1\Sigma_u^+$	0.6			>0.99	
$G\,^3\Pi_u$			2.3[b]		
$F\,^3\Pi_u$			1.2[b]		

[a]Reference 46.
[b]Average of cross section values given at 40 and 60 eV.

in the implied predissociation branching ratios (η_{dis}) for most of the states. The exception is the implied branching ratio for the c' state, which Zipf and McLaughlin find to be ~28% predissociated, while Ajello *et al.* find no evidence of predissociation, implying <10% predissociation considering the nominal accuracy of the emission cross sections. As pointed out by Ajello *et al.*, this disagreement would be even greater (55% vs <10%) if the Zipf and McLaughlin emission cross sections were rescaled to the new value for the Lyman-α standard.

Apart from the seven perturbed electronic states, excitation of several other electronic states that lie above the lowest dissociation limit is known to accompany electron impact on N_2. In particular, the $a\,^1\Pi_g$, $w\,^1\Delta_u$, $C\,^3\Pi_u$, $E\,^3\Sigma_g^+$, $a''\,^1\Sigma_g^+$, $G\,^3\Pi_u$, and $F\,^3\Pi_u$ states have measurable excitation cross sections.[8] The C state however, does not dissociate for levels that are significantly populated by electron impact,[44] and the strongly populated levels in both the a'' and E states are relatively long lived.[35,45] Both the a and w states are known to dissociate[44] in those levels, $v>6$ and $v>4$ respectively, that lie above the $N(^4S)+N(^4S)$ limit. Ajello and Shemansky[46] estimate that dissociation of the a state amounts to 13% of its excitation cross section and give values for the dissociation cross section of this state of 1.54, 0.77, and 0.39 Mb at electron energies of 50, 100, and 200 eV, respectively. The excitation cross section of the w state is large for threshold electron energies, but decreases rapidly with higher electron energies.[8] Its contributions to dissociation would be negligible at the higher electron energies. Emission has never been detected from either the G or F states, hence dissociation of these states is probable. Total excitation cross sections[8] for these states are 1.7 and 1.0 Mb, respectively, at 60 eV.

Predissociation of a rovibrational level produces a discrete release of translational energy to the fragment atoms which must be accounted for in describing electron energy deposition in N_2. Furthermore, both the translational energy and the electronic state of the dissociation fragment can affect its subsequent reactions. The magnitude of the translational energy release depends only on the energy of

the predissociated level above the relevant dissociation limit of the molecule. As discussed above, there are only three possible dissociation limits that can be populated from the b, b', c, c', e, and e' states. If fragments are formed at each of these limits, then one predissociated level can produce as many as three discrete translational energy releases which are widely separated in energy. Relative to the translational energy release for the production of ground state atoms $N(^4S)+N(^4S)$, the translational energy release for production of $N(^2D)+N(^4S)$ would be 2.384 eV lower, while that for production of $N(^2P)+N(^4S)$ would be 3.576 eV lower, given the known[47] energy separations of the atomic states.

The fragment energy release distributions observed in the present work from electron impact dissociation of N_2 provide a direct measure of the dissociation products from the ensemble of electronic states and rovibrational levels formed in the electron impact. Given that the relative predissociation cross sections for the dominant electronic states excited by electron impact are known (Table III), the distribution of fragment energy release accompanying their predissociation should be predictable with only a presumption as to which of the three possible dissociation limits are populated. Predicted fragment energy release distributions are shown in Fig. 4 together with observed distribution for 50 eV electron impact. The predicted distributions represent the partial dissociation cross sections for 100 eV electron impact of Ajello *et al.*[12] and James *et al.*[43] for the c', c, b', b, and o states, and of Ajello and Shemansky[46] for the a state. The partial dissociation cross sections for the e and e' states are the 200 eV partial excitation cross sections of Zipf and McLaughlin[11] and those for the G and F states are the 50 eV integral excitation cross sections of Trajmar *et al.*[8] distributed over vibrational envelopes characteristic of the $N_2^+X\,^2\Sigma_g^+$ and $A\,^2\Pi_u$ states, respectively. The energy of each point in the distribution represents a vibrational energy above the specified dissociation limit. An explicit consideration of rotational structure would smear these points to higher energy by 0.04 to 0.08 eV whereas apparatus resolution would broaden the rotational distribution by Eq. (3). The center distribution presumes that all predissociation, with the exception of the a state, produces $N(^2D)+N(^4S)$, while the bottom distribution is for production of $N(^2P)+N(^4S)$. In all cases, only the lowest dissociation limit is accessible in the predissociation of the a state. The $N(^4S)+N(^4S)$ and $N(^2D)+N(^2D)$ distributions are not shown. The former can be obtained by shifting all points in the center distribution, with the exception of those for state a, by $+2.746$ eV. The latter can be obtained by shifting the value of W for all points in the bottom distribution, also with the exception of a, by -1.191 eV. Very few of the known predissociated levels lie above the $N(^2D)+N(^2D)$ limit.

A comparison of the experimental fragment energy distribution with the calculated distributions shows a strikingly good agreement with that calculated for $N(^2D)+N(^4S)$ production. In particular, the two peaks in the experimental distribution match quite precisely with the production of fragments to this limit from $c(v=0)$ and $c(v=1)$, shown as the open squares in the center distribution with $W=0.797$ eV and $W=1.071$ eV, respectively. This association is made more compelling by the fact that vibrational excitation in the N_2 beam produced an enhanced intensity in the $W\sim 1.1$ eV peak, as was shown in Fig. 2. Furthermore a broadening of the lower W peak correlates with significant predissociation expected from $v=2,3,4$ of the b state. Finally, the sharp decrease in the experimental fragment intensity for $W>2.4$ eV is also matched by the relative predissociation cross sections, where the contribution here is largely from very high vibrational levels of the b' state.

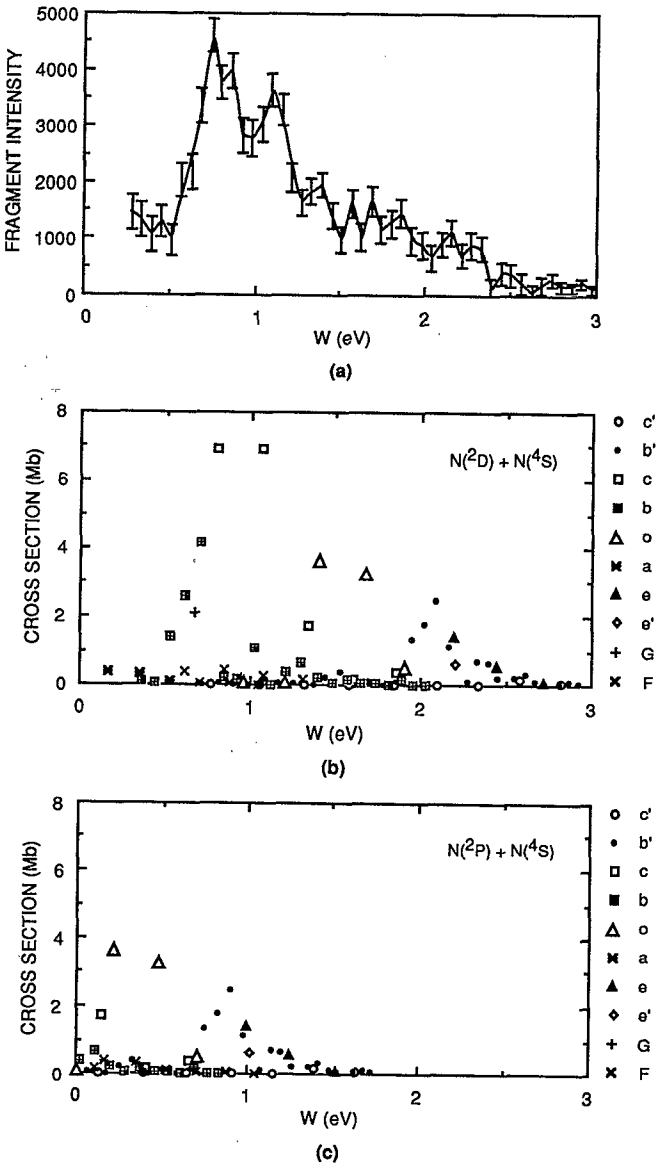

FIG. 4. Observed and predicted translational energy release distributions in the electron impact dissociation of N_2. The upper distribution is the translational energy release distribution observed for 48.5 eV electron impact. Distributions at the center and bottom of the figure are the partial dissociation cross sections for the vibrational levels of ten predissociated electronic states of N_2 (see the text and Table III) plotted as a function of energy relative to the $N(^2D)+N(^4S)$ dissociation limit (center) or the $N(^2P)+N(^4S)$ dissociation limit. The close correspondence between the top and center distributions indicates that $N(^2D)+N(^4S)$ are the dominant N_2 dissociation products.

The very good overall agreement between the center distribution and the experimental spectrum in Fig. 4 provides a clear indication that production of $N(^2D)+N(^4S)$ is the dominant dissociation channel in N_2 dissociation. Furthermore the experimental spectrum specifically excludes any significant production of $N(^4S)+N(^4S)$ dissociation products, except those arising from high vibrational levels of the a state. Of the remaining electronic states, the lowest energy level lies 2.746 eV above this dissociation limit. It can be seen from the experimental spectrum that very few fragments are produced at this or higher values of W. Finally, the experimental distribution clearly allows production of $N(^2P)+N(^4S)$ as a minor dissociation channel in the predissociation. As can be seen in Fig. 4, production of fragments at this limit will primarily contribute to the fragment energy distribution in the region near $W=1$ eV and would not be distinctly resolved as a minor contribution to the experimental spectrum. Information on the relative contributions of the ^2D and ^2P predissociation channels could in principle be determined from a quantitative simulation of the experimental fragment distributions. However, such a simulation is not attempted here. Rotationally resolved photofragment energy release studies have demonstrated that branching of the predissociation products between the ^2D and ^2P limits can be quite complex, as expected from the strong Rydberg–valence couplings, and must be considered on a level by level basis.[20] In particular, branching between these limits was shown to vary with rotational level for the $e'(v=0)$ state and with rotational level and parity for the $e(v=0)$ state. In contrast, the $b'(v=16,17)$ levels were found to exclusively ($>95\%$) predissociate to the $^2D + {}^4S$ limit, even though they lie more than 1 eV above the $^2P + {}^4S$ dissociation limit. These b' levels correspond to the solid circles in the center distribution at $W=2.091$ eV and 2.167 eV, respectively. Similar product branching determinations are in progress for the other N_2 states.[34]

Another conclusion from the comparison in Fig. 4 is that predissociation of bound N_2 states, as implied by the absence of significant continua in electron energy loss excitation spectra, makes the dominant contribution to the electron impact dissociation of N_2. Predissociation is consistent with the observed lack of sensitivity of the dissociation cross section to anticipated changes in the vibrational distribution within the N_2 beam. Furthermore, the overall pattern of predissociation among the N_2 states derived by Ajello *et al.*[12] and by James *et al.*[43] appears to be in rather good agreement with the observed fragment energy distributions. One might therefore expect that the sum of the partial dissociation cross sections of Ajello *et al.* and James *et al.* would approach the total dissociation cross sections determined in the present work and by Winters.[9] As shown in Table III, the sum of the dissociation cross sections for the b, b', c, c', o, and a states is 46.7 Mb with an absolute uncertainty of order 25%. Excitation and complete dissociation of the e, e', G, and F states would account for an additional ~ 6 Mb for the dissociation cross section to give a nominal total of 53 ± 18 Mb, where the error limits allow a factor of two uncertainty in the contributions of the latter states. The total dissociation cross section implied by the present measurements (Table I) is 85 ± 24 Mb. Thus these two sets of measurements are consistent within their nominal absolute uncertainties. However, the total dissociation cross section of Winters, $145+15/-29$ Mb, clearly is inconsistent with the summed partial dissociation cross sections, even allowing for an additional error contribution from uncertainty in the dissociative ionization correction. If we presume that both the Winters cross section and the summed partial dissociation cross sections are accurate within the stated limits, this would imply that dissociation channels, beyond those considered in Fig. 4, must contribute an additional >45 Mb to the dissociation, i.e., an increase of roughly a factor of 2 in both density and magnitude over the partial cross sections shown in Fig. 4. Although such a possibility cannot be excluded entirely, it does not seem reasonable given the good overall agreement shown in Fig. 4. More likely the discrepancies reflect the combined systematic errors in all three absolute cross sections. This would support the suggestion in the previous section that a weighted average of the total dissociation cross section determined by Winters and that determined in the present work will likely provide the most accurate measure for N_2 dissociation.

SUMMARY

Absolute dissociation cross sections and translational energy release distributions are measured for electron impact on N_2 in a fast molecular beam. The dissociation is observed without contamination of the products by the dissociative ionization channel. A comparison of the observed fragment distributions with the known energies and partial dissociation cross sections of excited levels of N_2 indicates that predissociation to form $N(^2D)+N(^4S)$ products is the dominant dissociation mechanism. Production of $N(^4S)+N(^4S)$ and $N(^2P)+N(^4S)$ as minor dissociation channels cannot be excluded on the basis of the present measurements.

Absolute cross sections measured in the present experiment are found to be consistent with those previously determined by Winters. A combination of the present values with previous measurements of the absolute and relative dissociation cross sections yields a set of recommended values for the N_2 dissociation cross section over the electron energy range from 10 to 200 eV. Given the vast differences in technique among the various measurements, the recommended values (Table II) should be considered highly reliable within their stated absolute uncertainties.

ACKNOWLEDGMENT

This research was supported by the U.S. Air Force Wright Laboratory under Contract No. F33615-85-R-2560.

[1] J. L. Fox and G. A. Victor, Planet. Space Sci. **36**, 329 (1988); D. F. Strobel, R. R. Meier, M. E. Summers, and D. J. Strickland, Geophys. Res. Lett. **18**, 689 (1991).

[2] D. Rapp and P. Englander-Golden, J. Chem. Phys. **43**, 1464 (1965).

[3]P. B. Armentrout, S. M. Tarr, A. Dori, and R. S. Freund, J. Chem. Phys. **75**, 2786 (1981).
[4]J. P. Doering and L. Goembel, J. Geophys. Res. **96**, 16025 (1991).
[5]D. Rapp, P. Englander-Golden, and D. D. Briglia, J. Chem. Phys. **43**, 4081 (1965).
[6]A. Crowe and G. W. McConkey, J. Phys. B **6**, 2108 (1973).
[7]K. Kollmann, Int. J. Mass Spectrom. Ion Phys. **17**, 261 (1975).
[8]S. Trajmar, D. F. Register, and A. Chutjian, Phys. Rep. **97**, 219 (1983).
[9]H. F. Winters, J. Chem. Phys. **44**, 1472 (1966).
[10]A. Niehaus, Z. Naturforsch. Teil A **22**, 690 (1967).
[11]E. C. Zipf and R. W. McLaughlin, Planet. Space Sci. **26**, 449 (1978).
[12]J. M. Ajello, G. K. James, B. O. Franklin, and D. E. Shemansky, Phys. Rev. A **40**, 3524 (1989).
[13]Y. Itikawa, M. Hayashi, A. Ichimura, K. Onda, D. Sakimoto, K. Takayanagi, M. Nakamura, H. Nishimura, and T. Takayanagi, J. Phys. Chem. Ref. Data **15**, 985 (1986).
[14]S. Solomon, Planet. Space Sci. **31**, 135 (1983).
[15]J. Geiger and B. Schröder, J. Chem. Phys. **50**, 7 (1969).
[16]G. Joyez, R. I. Hall, J. Reinhardt, and J. Mazeau, J. Electron Spectrosc. Relat. Phenom. **2**, 183 (1973).
[17]A. Chutjian, D. C. Cartwright, and S. Trajmar, Phys. Rev. A **16**, 1052 (1977).
[18]P. Hammond, G. C. King, J. Jureta, and F. H. Read, J. Phys. B **20**, 4255 (1987).
[19]D. Stahel, M. Leoni, and K. Dressler, J. Chem. Phys. **79**, 2541 (1983).
[20]H. Helm and P. C. Cosby, J. Chem. Phys. **90**, 4208 (1989).
[21]E. C. Zipf, P. J. Espy, and C. F. Boyle, J. Geophys. Res. **85**, 687 (1980).
[22]D. W. Rusch and J.-C. Gerard, J. Geophys. Res. **85**, 1285 (1980).
[23]P. C. Cosby, J. Chem. Phys. **98**, 7804 (1993).
[24]H. Helm and P. C. Cosby, J. Chem. Phys. **86**, 6813 (1987).
[25]D. P. deBruijn and J. Los, Rev. Sci. Instrum. **53**, 1020 (1982).
[26]R. C. Wetzel, F. A. Baiocchi, T. R. Hayes, and R. S. Freund, Phys. Rev. A **35**, 559 (1987).
[27]H. Helm, Phys. Rev. A **38**, 3425 (1988).
[28]C. W. Walter, P. C. Cosby, and J. R. Peterson, J. Chem. Phys. **98**, 2860 (1993).
[29]F. R. Gilmore, R. R. Laher, and P. J. Espy, J. Phys. Chem. Ref. Data **21**, 1005 (1992).
[30]P. C. Cosby and H. Helm, Phys. Rev. Lett. **61**, 298 (1988).
[31]M. R. Flannery, P. C. Cosby, and T. F. Moran, J. Chem. Phys. **59**, 5494 (1973).
[32]M. R. Flannery and T. F. Moran, J. Phys. B **9**, L509 (1976).
[33]W. J. van der Zande, W. Koot, J. R. Peterson, and J. Los, Chem. Phys. Lett. **140**, 175 (1987).
[34]C. W. Walter, P. C. Cosby, and H. Helm, Bull. Am. Phys. Soc. **37**, 1099 (1992); J. Chem. Phys. (submitted for publication).
[35]A. W. Kam and F. M. Pipkin, Phys. Rev. A **43**, 3279 (1991).
[36]H. F. Winters, D. E. Horne, and E. E. Donaldson, J. Chem. Phys. **41**, 2766 (1964).
[37]T. Nakano, H. Toyoda, and H. Sugai, Jpn. J. Appl. Phys. **30**, 2908, 2912 (1991).
[38]E. C. Zipf, in *Electron–Molecule Interactions and Their Applications*, edited by L. G. Christophorou (Academic, Orlando, 1984) V. I, Chap. 4.
[39]J. M. Ratliff, G. K. James, S. Trajmar, J. M. Ajello, and D. E. Shemansky, J. Geophys. Res. **96**, 17559 (1991).
[40]Y. Roncin, F. Launay, and M. Larzilliere, Phys. Rev. Lett. **53**, 159 (1984).
[41]K. P. Huber and Ch. Jungen, J. Chem. Phys. **92**, 850 (1990).
[42]D. E. Shemansky, J. M. Ajello, and D. T. Hall, Ap. J. **296**, 765 (1985).
[43]G. K. James, J. M. Ajello, B. Franklin, and D. E. Shemansky, J. Phys. B **23**, 2055 (1990).
[44]A. Lofthus and P. H. Krupenie, J. Phys. Chem. Ref. Data **6**, 113 (1977).
[45]R. S. Freund, J. Chem. Phys. **50**, 3734 (1969).
[46]J. M. Ajello and D. E. Shemansky, J. Geophys. Res. **90**, 9845 (1985).
[47]C. E. Moore, Natl. Stand. Ref. Data Ser., Natl. Bur. Stand. (U.S.) **34** (Sept. 1970).